

DYNAMICS OF THE REACTION S(¹D) + HD, H₂, AND D₂: ISOTOPIC BRANCHING RATIOS AND TRANSLATIONAL ENERGY RELEASE

YOUSUKE INAGAKI, SAYED MOHAMMED SHAMSUDDIN,
YUTAKA MATSUMI and MASAHIRO KAWASAKI

*Institute for Electronic Science and Graduate School of Environmental Earth
Science, Hokkaido University, Sapporo 060, Japan*

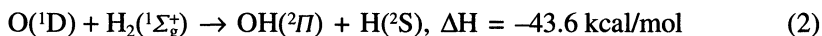
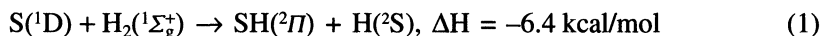
(Received 20 June, 1993)

Doppler profiles of H and D atoms from the reaction S(¹D) with HD and a 1 : 1 mixture of H₂ and D₂ have been measured by a laser-induced fluorescence technique with a vacuum ultraviolet laser. An isotopic channel branching ratio of ϕ (SD + H)/ ϕ (SH + D) is measured to be 0.9 ± 0.1 in the reaction of S(¹D) + HD at average collision energy $E_{\text{coll}} = 1.2$ kcal/mol. In S(¹D) + HD, D₂, and H₂, the translational energies released are almost the same, 4.6 ± 0.5 kcal/mol for H and D production channels. The measured branching ratio and translational energy release suggest that the reaction proceeds via a long-lived complex formed by insertion.

KEY WORDS: Doppler profile, S(¹D) atom, isotopic branching ratio, translational energy, reaction dynamics.

INTRODUCTION

An atom-diatomic molecular reactive scattering is one of the fundamental elementary chemical reactions. Among them, the system for an atom, S and O, in the electronically excited singlet state,

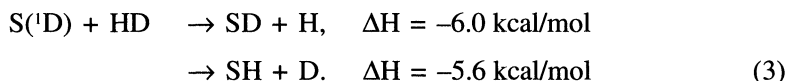


has drawn much attention for many years because this system provides several particularly interesting features in the study of reaction dynamics. This system is characterized by a deep potential minimum corresponding to H₂O or H₂S on its X¹A₁ surface that is directly associated to the reagents.¹

Given these features, numerous experimental and theoretical studies have been performed to understand the dynamics of the reaction particularly for the O(¹D) + H₂ system.² Previous measurements on internal energy distributions and the angular distributions of the OH products largely support an insertion mechanism for

this reaction.³⁻⁵ Of particular importance among the measurements is the isotopic branching $[H]/[D]$ ratio, which denotes the channel branching ratio $\phi(\text{OD} + \text{H})/\phi(\text{OH} + \text{D})$ from the reaction of $\text{O}(^1\text{D})$ with HD. A measurement using a laser-induced fluorescence (LIF) detection of H/D atoms with vacuum ultraviolet (VUV) laser light at a low collision energy ($E_{\text{coll}} = 2.4\text{--}3.4$ kcal/mol) reported the ratio of 1.13 ± 0.08^6 or $1.4 \pm 0.3.^7$ Theoretical ratio $\phi(\text{OD} + \text{H})/\phi(\text{OH} + \text{D})$ varies from 1.1 ~ 2.3, depending on what surface is used^{8,9} because the ratio is very sensitive to the shape of the surface. Extensive theoretical studies and the recent measurements of the vibrational energy distribution of the OH product predict a very short-lived complex because of its large exoergicity.

On the other hand, detailed dynamics of the $\text{S}(^1\text{D}) + \text{H}_2$ reaction are still ambiguous. Since the $\text{S}(^1\text{D}) + \text{H}_2$ reaction has much smaller exoergicity than $\text{O}(^1\text{D}) + \text{H}_2$, comparison of these two isoelectronic reactions reveals a different detailed dynamics. In this paper, we report the reactions of $\text{S}(^1\text{D})$ with H_2 , D_2 , or HD at a low collision energy using a vacuum-UV LIF technique which enables the measurement of the Doppler profiles of H and D spectra so that the average kinetic energies of the products can be calculated:



EXPERIMENT

The experimental setup used is shown in Figure 1. The $[H]/[D]$ ratios and Doppler profiles from $\text{S}(^1\text{D}) + \text{HD}$ were measured with a LIF method at 121.6 nm. Premixed CS_2 and HD (H_2 , D_2) gas flowed into a reaction cell. The cell, $60 \times 60 \times 60$ mm, was pumped by a rotary pump and a liquid nitrogen trap. The pressures of CS_2 and HD in the reaction cell were typically 5 and 60 mTorr, respectively. ArF excimer laser light at 193 nm (~ 2 mJ/pulse, 10 Hz) dissociated CS_2 and produced translationally hot $\text{S}(^1\text{D})$ atoms. 200 ns after the firing the photolysis laser pulse, a probe vacuum-UV laser was fired to detect H and D atoms produced from the reaction. The two laser beams of the photolysis and probe were perpendicularly crossed with each other. The probe light for H and D atoms around 121.6 nm was generated by four-wave mixing using a $2\omega_1 - \omega_2$ scheme in a Kr gas cell¹⁰ with two tunable dye lasers pumped by a XeCl excimer laser (308 nm, 240 mJ/pulse). The output of the vacuum-UV light going through the reaction cell was monitored with a vacuum-UV monochromator and a solar-blind photomultiplier. The laser induced fluorescence was observed by another solar-blind photomultiplier at right angles to both the photolysis and probe laser beams passing through a LiF window and a band-pass filter (Acton Research, $\lambda = 120$ nm, $\Delta\lambda = 12$ nm). The delay (200 ns) between the photolysis and probe light pulses was controlled with a time jitter of about 10 ns. Since the beam diameter of the photolysis laser was large enough, within a 200 ns delay the reactions were presumed to proceed

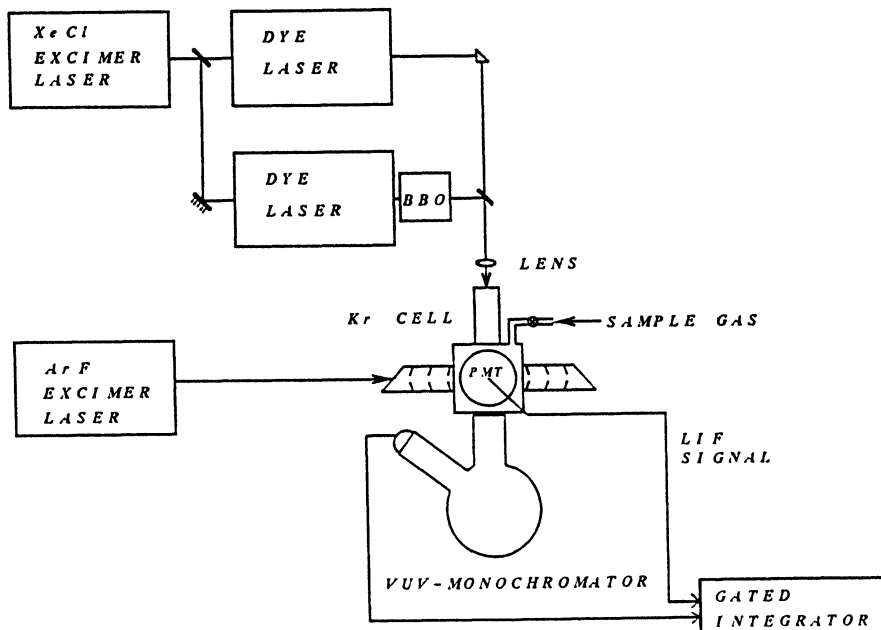


Figure 1 Experimental setup for laser induced fluorescence measurement of H and D atoms at 121.6 nm.

homogeneously in the probing region and escape of the products from the viewing zone could be ignored. Therefore, the measured concentration ratios $[H]/[D]$ are equal to the channel branching ratios of the reaction $\phi(SD + H)/\phi(SH + D)$ for the reaction of $S(^1D)$ with HD.

In the experiments for the spatial distribution of the H atom velocity, the output of the photolysis laser was polarized with a pile-of-plates polarizer. Doppler profiles were measured in the two configurations of $\hat{E}_d // \hat{k}_p$ and $\hat{E}_d \perp \hat{k}_p$, where \hat{E}_d is the polarization vector of the linearly polarized dissociation laser light and \hat{k}_p is the propagation direction of the probe laser. The dye laser for the dumping light ω_2 was installed with an intracavity etalon so that the spectral width was narrowed. In order to test the spectral resolution of our system, the Doppler spectra of the product D atoms were measured with Ar (2 Torr) added. While the theoretical thermal Doppler width is as narrow as 0.65 cm^{-1} , the measured full width at half maximum was 0.92 cm^{-1} that was expected for a D atom with $T = 300 \text{ K}$, considering that the splitting of the upper electronic states $\Delta E(^2P_{1/2} - ^2P_{3/2})$ is 0.37 cm^{-1} and the spectral width of the probe laser light is 0.34 cm^{-1} . Spectral width was broadened by a factor of 1.4 for the D atomic line at 300 K. Spectral broadening due to these terms is not large for the product H and D atoms from $S(^1D) + H_2, D_2$ and HD because H and D atoms have typical Doppler widths of 3 and 2 cm^{-1} , respectively. The translational energy data were corrected for this broadening and the change was less than 5%.

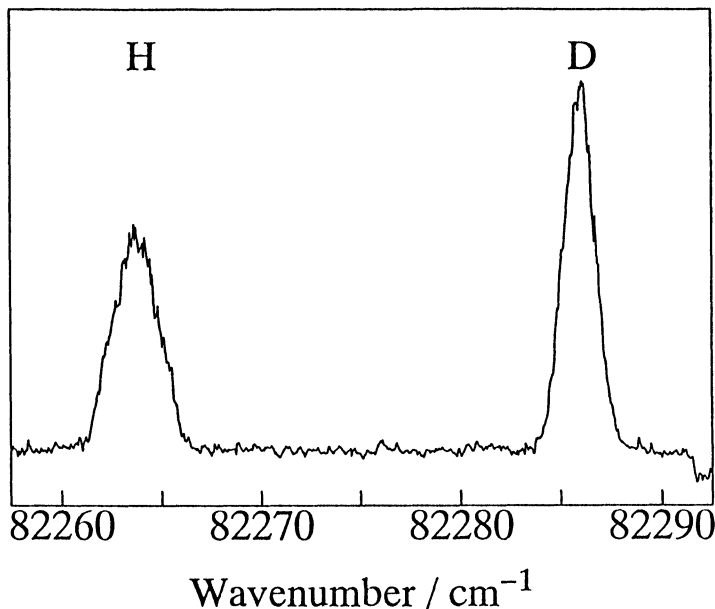


Figure 2 LIF spectra of H and D atoms produced from the reaction of S(¹D) with HD (60 mTorr). S(¹D) atoms are produced by photodissociation of CS₂ (10 mTorr) at 193 nm.

RESULTS

The typical vacuum-UV LIF spectra of the H and D atoms produced from the reaction of S(¹D) with HD are shown in Figure 2. The isotopic ratio [H]/[D] is calculated to be 0.9 ± 0.1 for S(¹D) + HD from the obtained spectra and listed in Table I. This ratio is in good agreement with the reported ratio, ca.1.⁶ The ratio [H]/[D] for the reaction O(¹D) + HD is also listed in Table I for comparison purpose.⁷

Table I Isotopic branching ratios for S(¹D) + HD and O(¹D) + HD.

	$\langle E_{\text{coll}} \rangle^{\text{a}}$	$[H]/[D]^{\text{b}}$		Ref.
	kcal/mol	Experimental	Theoretical ^c	
S(¹ D)	1.2	0.9 ± 0.1	0.89	This work 6
	1.2	ca.1		
O(¹ D)	2.4	1.5 ± 0.2	1.01	7

a. Average center-of-mass collision energy for the reaction of S(¹D) and O(¹D) with HD.

b. Measured [H]/[D] product concentration ratios. The values correspond to isotopic channel ratios $\phi(\text{AD} + \text{H})/\phi(\text{AH} + \text{D})$. Numbers in parentheses are errors (one sigma).

c. Statistical model Eq. (9), using average collision energies.

With a linearly polarized photolysis laser at 193 nm, the measured Doppler profiles of the H(D) atoms were identical to each other for the two polarization configurations of $\hat{E}_{\text{d}} // \hat{k}_{\text{p}}$ and $\hat{E}_{\text{d}} \perp \hat{k}_{\text{p}}$. This indicates that the angular distributions of the H and D

atoms are almost isotropic in the laboratory (LAB) frame although an anisotropic angular distribution is expected for the reactant S(¹D) atoms produced from photodissociation of CS₂ by the polarized 193 nm laser light. Therefore, we assumed an isotropic velocity distribution for the H and D atoms in the LAB frame. The average kinetic energies of the H and D atoms in the laboratory frame were calculated from Figure 2 with the second moment $\langle v^2 \rangle$ of the observed Doppler profiles and then converted to the total kinetic energy released to the products in the center-of-mass (c.m.) frame $\langle E'_t \rangle$.¹¹ A second moment of the Doppler profiles of a product atom is given by the following equation:

$$\langle v^2 \rangle = c^2 \int_{-\infty}^{\infty} [(\nu - \nu_0)/\nu_0]^2 g(\nu) d\nu, \quad (4)$$

where $g(\nu)$ is the normalized Doppler profile, ν the frequency of the probe laser, and ν_0 the resonance center frequency.

The average translational energy $\langle E'_t \rangle$ released to the products in the c.m. frame can be calculated from the average translational energy $\langle E_t^{\text{LAB}}(\text{H}) \rangle$ of the H atoms in the LAB frame:

$$\begin{aligned} \langle E_t^{\text{LAB}}(\text{H}) \rangle &= (3m(\text{H})/2)\langle v^2(\text{H}) \rangle, \\ &\simeq \langle E'_t \rangle m(\text{SH})/m(\text{H}_2\text{S}) + \langle E_t^{\text{LAB}}(\text{H}_2\text{S}) \rangle m(\text{H})/m(\text{H}_2\text{S}), \end{aligned} \quad (5)$$

for the S(¹D) + H₂ reaction system, where $\langle E_t^{\text{LAB}}(\text{H}_2\text{S}) \rangle$ is the kinetic energy for the c.m. of the reaction system in the LAB frame. $\langle E_t^{\text{LAB}}(\text{H}_2\text{S}) \rangle$ is given by

$$\langle E_t^{\text{LAB}}(\text{H}_2\text{S}) \rangle = \langle E_t^{\text{LAB}}(\text{S}) \rangle m(\text{S})/m(\text{H}_2\text{S}) + \langle E_t^{\text{LAB}}(\text{H}_2) \rangle m(\text{H}_2)/m(\text{H}_2\text{S}), \quad (6)$$

The values of $\langle E_t^{\text{LAB}}(\text{H}_2\text{S}) \rangle m(\text{H})/m(\text{H}_2\text{S})$ in eq. (5), which correspond to the contribution of the motion of the center-of-mass, are 0.1–0.2 kcal/mol. The obtained values of $\langle E'_t \rangle$ are listed in Table II. For calculation, the laser width ($\sim 0.34 \text{ cm}^{-1}$ at 121.6 nm) and the splitting of the upper H(²P_i) levels (0.37 cm^{-1}) were taken into account. An example of the curve fitting procedure of the Doppler profile is shown in Figure 3 for the D atom from the reaction S(¹D) + D₂. The broken line represents each component of the D(²P_{1/2}) ← D(²S) and D(²P_{3/2}) ← D(²S) transition, and the solid line is a sum of these components that fits with the experimentally obtained Doppler profile. This correction reduced the $\langle v^2 \rangle$ value by ca. 5%. The $\langle E'_t \rangle$ values are almost equal among the reactions with HD, H₂, and D₂ as shown in Table II.

The average fraction of the total available energy which is released as translation is defined as $\langle f'_t \rangle = \langle E'_t \rangle / \langle E_{\text{avl}} \rangle$. For calculation of $\langle E_{\text{avl}} \rangle$, one must know the collision energy. The average c.m. collision energies E_{coll} for the S(¹D) + AB reaction (AB: H₂, D₂ or HD) are calculated with the following equation,¹²

$$\langle E_{\text{coll}} \rangle = \frac{1}{2} \frac{m(\text{AB})m(\text{S})}{m(\text{AB}) + m(\text{S})} \left[\frac{2}{m(\text{S})} \langle E_t^{\text{LAB}}(\text{S}) \rangle + \frac{2}{m(\text{AB})} \cdot \frac{3}{2} kT \right], \quad (7)$$

Table II Translational energies for S(¹D) or O(¹D) + HD, H₂, and D₂.

Reaction	$\langle E_{\text{avl}} \rangle^a$	$\langle E_{\text{t}}' \rangle^b$	$\langle f_{\text{t}}' \rangle^c$	
	kcal mol ⁻¹		Experimental	Theoretical ^d
S(¹ D) + HD → SD + H	7.2	4.7 ± 0.6	0.65 ± 0.15	0.54
S(¹ D) + HD → SH + D	6.8	4.2 ± 0.7	0.61 ± 0.12	0.60
S(¹ D) + H ₂ → SH + H	7.6	4.3 ± 0.2	0.57 ± 0.02	0.59
S(¹ D) + D ₂ → SD + D	6.3	4.1 ± 0.3	0.65 ± 0.05	0.57
O(¹ D) + HD → OD + H	46.5	20 ± 4	0.43 ± 0.09	0.45
O(¹ D) + HD → OH + D	45.1	10 ± 2	0.22 ± 0.04	0.47
O(¹ D) + H ₂ → OH + H	45.5	15 ± 3	0.33 ± 0.07	0.47
O(¹ D) + D ₂ → OD + D	46.0	14 ± 3	0.30 ± 0.07	0.45

- Averaged available energy, $\langle E_{\text{coll}} \rangle + \Delta H$. The Heat of Reaction is calculated based on the data ΔH_{298} from Refs. 14 and 15. $\langle E_{\text{coll}} \rangle$ for the S(¹D) reactions is given in the text. $\langle E_{\text{coll}} \rangle$ for the reactions of O(¹D) with HD, H₂, and D₂ are 2.4, 1.9, 2.8 kcal/mol⁻¹, respectively.
- Averaged center-of-mass translational energy released to the product, which is obtained from the second moment of the Doppler profile of H or D atoms. Numbers in parentheses are errors (one sigma).
- Fraction of the translational energy to the total available energy, $\langle f_{\text{t}}' \rangle = \langle E_{\text{t}}' \rangle / \langle E_{\text{avl}} \rangle$.
- Statistical calculation using Eqs. (8) and (10).

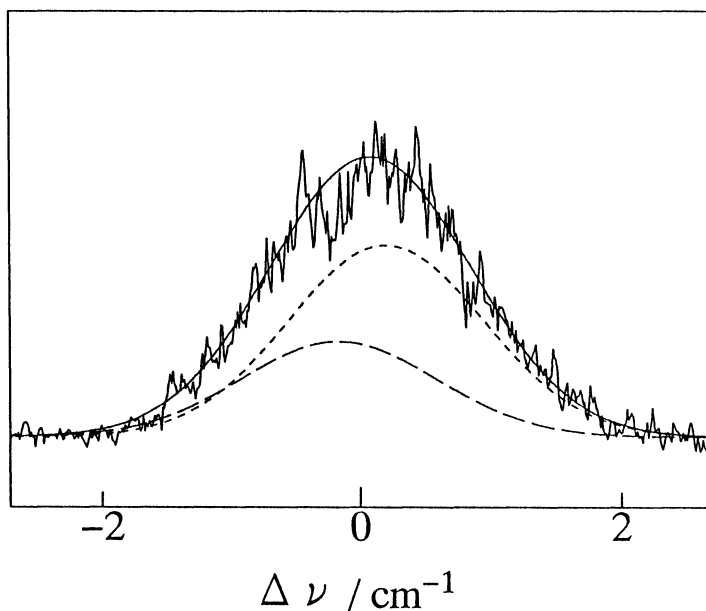


Figure 3 LIF spectra of D atoms produced from S(¹D) + D₂. The solid line is the best-fit of the simulated curve that is a sum of two Gaussian curves. A full width at half maximum (FWHM) of the probe laser is 0.34 cm⁻¹ and the splitting in the upper D(²P_{3/2}, _{1/2}) level is 0.37 cm⁻¹. A dotted line is a simulated curve with FWHM = 1.74 cm⁻¹ for each component of the D(²P_{1/2}) – D(²S) and D(²P_{3/2}) – D(²S) transitions.

where $m(i)$ refers to a mass of the i reactant and T is room temperature. $\langle E_t^{\text{LAB}}(S) \rangle$ is the average translational energy in the LAB frame for the S(¹D) atoms which are produced in the photolysis of CS₂ at 193 nm. The average kinetic energy of S(¹D) from CS₂ at 193 nm has been reported to be 4.8 kcal/mol by McCrary *et al.*¹³ The estimated collision energies $\langle E_{\text{coll}} \rangle$ are 1.2, 1.3, and 1.1 kcal/mol for S(¹D) + HD, D₂, and H₂. The average available energy is obtained by $\langle E_{\text{AVL}} \rangle = \langle E_{\text{coll}} \rangle + \Delta H$ as shown in Table II. In this calculation the heat of formation used for $\Delta H(\text{SD}) = 34.61$ kcal/mol, $\Delta H(\text{SH}) = 34.10$ kcal/mol, $\Delta H(\text{OD}) = 8.81$ kcal/mol, $\Delta H(\text{OH}) = 9.31$ kcal/mol, $\Delta H(\text{S}(\text{}^1\text{D})) = 92.62$ kcal/mol, $\Delta H(\text{H}) = 52.09$ kcal/mol, and $\Delta H(\text{D}) = 52.98$ kcal/mol.^{14,15} Using these $\langle E_{\text{AVL}} \rangle$ values, the fractions of the total available energy released into translation are calculated and listed in Table II. For comparison purpose, the fractions $\langle f_t^i \rangle$ for O(¹D) + HD, H₂, and D₂ are also listed in Table II.

DISCUSSION

A. [H]/[D] Ratio and Reaction Mechanism

The measured [H]/[D] ratio for the reaction S(¹D) + HD is given in Table I, which is 0.9 ± 0.1 . Black and Jusinski¹⁶ reported that the rate constant for the S(¹D) + H₂ system is $k = 2.1 \times 10^{-10}$ cm³ molec⁻¹s⁻¹ at 300 K. This large rate constant suggests that reactant attraction is rather strong and leads to a complex. When considering product branching ratios from a hot complex, Zamir and Levine¹⁷ proposed the prediction of a statistical theory. The prior distribution of states in the products is of the form,

$$P^0(E_T, E_R, E_V | E_{\text{AVL}}) = (2J + 1) \rho_T(E_T) \times \delta(E_{\text{AVL}} - E_T - E_R - E_V) / \rho(E_{\text{AVL}}). \quad (8)$$

The density of translational states $\rho_T(E_T)$ is given as usual by $A_T E_T^{\frac{1}{2}}$ where $A_T = \mu^{\frac{3}{2}} / 2\pi^2 h^3$. $\rho(E_{\text{AVL}})$ is the total density of states and serves to normalize the prior distribution. In the present set of reactions A + HD, the rotational and vibrational levels of product hydrides are widely separated so that a summation over the discrete vibrational states is required for calculation of the state density.

$$[\text{H}]/[\text{D}] = \frac{\mu_{\text{AD,H}}^{\frac{3}{2}} \sum_{v=0}^{v_{\text{max}}} \sum_{J=0}^{J_{\text{max}}} (2J + 1) [E_{\text{AVL}}(\text{AD}) - E_{\text{AD}}(J, v)]^{\frac{1}{2}}}{\mu_{\text{AH,D}}^{\frac{3}{2}} \sum_{v=0}^{v_{\text{max}}} \sum_{J=0}^{J_{\text{max}}} (2J + 1) [E_{\text{AVL}}(\text{AH}) - E_{\text{AH}}(J, v)]^{\frac{1}{2}}}, \quad (9)$$

where J and v are the rotational and the vibrational quantum number, respectively. $\mu_{i,j}$ is the reduced mass of systems i and j . In the calculation of E_{AVL} , the averaged collision energies $\langle E_{\text{coll}} \rangle$ are calculated from the data of the translational energy reported by McCrary *et al.*¹³ Substituting the known spectroscopic data and E_{AVL} from Table II, calculated [H]/[D] ratios are 0.89 for S(¹D) + HD. Even if the translational energy distribution of S(¹D) atoms¹³ and the Boltzmann energy distribution of HD are taken into account, the calculated ratio [H]/[D] is almost the same as that

calculated with the average value $\langle E_{\text{coll}} \rangle$, probably because the range of distribution of the collision energy is as small as 1 kcal/mol. Our experimental result, 0.9 ± 0.1 for $\text{S}(^1\text{D}) + \text{HD}$ is in good agreement with the theoretical ratio, suggesting the formation of the complex. For comparison purpose, the isotopic branching ratio $[\text{H}]/[\text{D}]$ is also calculated for $\text{O}(^1\text{D}) + \text{HD}$ using eq. (9), which is 1.01. The reported experimental value was 1.5 ± 0.2 for the same collision energy.⁷ This difference between the theoretical and experimental values suggests nonstatistical behavior of the $\text{H}_2\text{O}^\ddagger$ complex.

B. Kinetic Energy Release And Reaction Mechanism

The detailed dynamics of the reaction can be understood from the internal energy and the isotropic angular distribution of the products. The deep potential well followed by a steep increase in the potential energy along the reaction coordinate favors a long-lived complex and a statistical energy distribution among the degrees of freedom of the products. As shown in Table II, the product translational energies $\langle E'_T \rangle$ for $\text{S}(^1\text{D}) + \text{HD}$, H_2 , and D_2 are almost equal to each other and show no isotope effect. On the other hand, in the reaction of $\text{O}(^1\text{D}) + \text{HD}$, the $\langle E'_T \rangle$ values for the $\text{OD} + \text{H}$ product channel are almost twice as high as those for the $\text{OH} + \text{D}$ channel. In addition, it should be noticed that the averaged value of $\langle E'_T \rangle$ over the $\text{OD} + \text{H}$ and $\text{OH} + \text{D}$ channels are almost equal to $\langle E'_T \rangle$ for $\text{O}(^1\text{D}) + \text{H}_2$ or $\text{O}(^1\text{D}) + \text{D}_2$ reactions. For both reaction systems of $\text{S}(^1\text{D})$ and $\text{O}(^1\text{D})$ with hydrogen (deuterium) molecules, an intermediate complex is formed: $\text{H}_2\text{S}^\ddagger(\text{X}^1\text{A}_1)$ and $\text{H}_2\text{O}^\ddagger(\text{X}^1\text{A}_1)$. The difference between these systems is in the available energies, that is, 7.6 kcal/mol for $\text{S}(^1\text{D}) + \text{H}_2$ and 45.5 kcal/mol for $\text{O}(^1\text{D}) + \text{H}_2$. Since the dissociation lifetime is determined by the velocity with which the complex passes over the activation region, $\text{H}_2\text{S}^\ddagger$ decomposes much more slowly than $\text{H}_2\text{O}^\ddagger$.

Most of the recent trajectory calculations predict a very short lifetime of the complex, shorter than one or two bending vibrational periods of the $\text{H}_2\text{O}^\ddagger$ complex.⁹ The short lifetime of the complex $\text{H}_2\text{O}^\ddagger$ would be expected because the system has a relatively small reduced mass upon which a large impulsive force is applied with large excess energy. Fitzcharles and Schatz⁹ presented a simple kinetic model for $\text{O}(^1\text{D}) + \text{HD}$ as follows. The $\text{O}(^1\text{D})$ atom preferably approaches at right angles to the HD molecular axis and the insertion takes place. The bending mode in the HDO^\ddagger complex is strongly excited. Before the vibrational energy in the bending mode is redistributed among other modes, a hard collision between the H and D atoms causes dissociation of the complex and the lighter H atom escapes the complex with higher probability. On the other hand, in the HSD^\ddagger complex that has only 6.8–7.2 kcal/mol as the available energy, the bending mode is not strongly excited. Hence, the vibrational energy is randomized in the long-lived HSD^\ddagger complex. Thus, the relative quantum yield of H and D is close to unity.

Energy partitioning in dissociation of an energized molecule is discussed in the framework of the statistical theory by Zamir and Levine.¹⁸ An average translational energy $\langle E_T \rangle$ is given by,

$$\langle E_T \rangle = \sum_{v=0}^{v_{\max}} \sum_{j=0}^{j_{\max}} E_T P^0(E_T, E_R, E_v | E_{\text{AVL}}). \quad (10)$$

With suitable molecular constants, the average translational energies for the reactions of S(¹D) + HD, H₂, D₂ are calculated using the average collision energies. The fraction $\langle f_T \rangle$ of the translational energy over the available energy is shown in Table II. Even if the translational energy distribution of S(¹D) is taken into account, based on the data by McCrary *et al.*¹³ for CS₂ photodissociation at 193 nm, $\langle f_T \rangle$ is the same as that calculated with the average $\langle E_{\text{coll}} \rangle$ value. For the case of S(¹D) + HD, H₂, and D₂, the statistical (prior) distribution well reproduces the $\langle f_T \rangle$ values. On the other hand, for O(¹D) + HD, H₂, D₂, the calculated $\langle f_T \rangle$ values are much larger than the experimental results. This result suggests that the reaction S(¹D) + H₂ proceeds through the insertion/decomposition pathway with a rather long dissociation lifetime of the complex, while the reaction of O(¹D) + H₂ follows the insertion/decomposition pathway within a period of the bending motion.⁹ The S(¹D) and O(¹D) atom insertion into the H₂ bond produces H₂S[‡] and H₂O[‡] with 98.6 and 165.1 kcal/mol internal excitation, respectively. A large fraction of the internal energy appears as large amplitude bending motion with the H₂S and H₂O intermediate undergoing inversion.

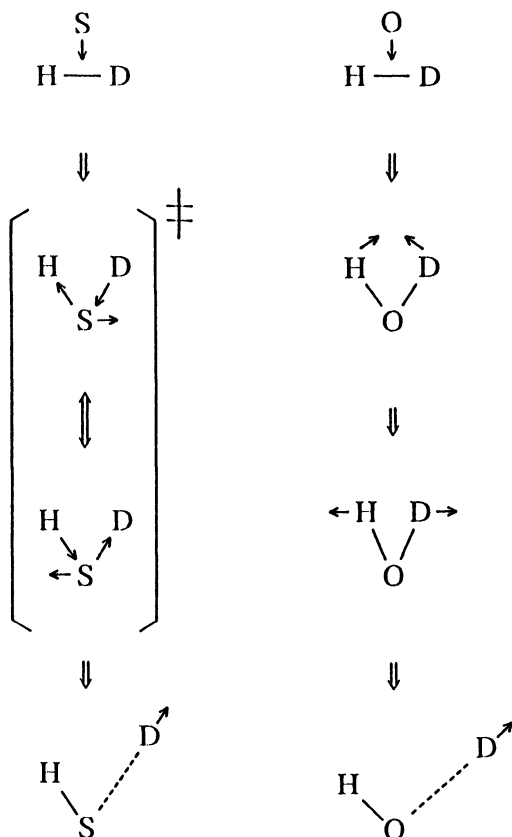


Figure 4 Schematics of insertion/decomposition mechanisms of S(¹D) + HD and O(¹D) + HD.

The dissociation mechanisms are schematically shown in Figure 4. During a relatively long lifetime of a HSD[‡] complex, the excess energy in this reaction is randomized almost completely and follows the statistical energy partition rule. However, in the HOD[‡] complex, a hard collision between the H and D atoms induces separation of the H or D atoms from the oxygen atom. The intermediate H₂O[‡] decomposes into OH + D or OD + H after this single bending vibration. An anisotropic angular distribution of the product OH was reported by Buss *et al.*⁵ in their molecular beam scattering experiment of O(¹D) + H₂.

Acknowledgement

This work is supported by the Grant-in-Aid from the Ministry of Education of Japan and the Matsuo Foundation.

References

1. P. A. Whitlock, J. T. Muckerman and E. R. Fisher. *J. Chem. Phys.*, **76**, 4468 (1982).
2. J. J. Sloan. *J. Phys. Chem.*, **92**, 18 (1988).
3. J. E. Butler, G. M. Jursich, J. A. Watson and J. R. Wiesenfeld. *J. Chem. Phys.*, **84**, 5365 (1986).
4. C. B. Cleveland, G. M. Jursich, M. Troler and J. R. Wiesenfeld. *J. Chem. Phys.*, **86**, 3253 (1987).
5. R. J. Buss, P. Casavecchia, T. Hirooka, S. J. Sibener and Y. T. Lee. *Chem. Phys. Lett.*, **82**, 386 (1981).
6. K. Tsukiyama, B. Katz and R. Bersohn. *J. Chem. Phys.*, **83**, 2889 (1985).
The [H]/[D] ratio reported in this reference was 1.9 but an additional unpublished experiment by G. Johnston and R. Bersohn showed that the ratio is close to one.
7. Y. Matsumi, K. Tonokura, M. Kawasaki and H. L. Kim. *J. Phys. Chem.*, **96**, 10622 (1992).
8. L. J. Dunne. *Chem. Phys. Lett.* **158**, 535 (1989).
9. M. A. Fitzcharles and G. C. Schatz. *J. Phys. Chem.*, **90**, 3634 (1986).
10. G. Hilber, A. Lago and R. Wallenstein. *J. Opt. Soc. Am.*, **B4**, 1753 (1987).
11. N. Shafer, K. Tonokura, Y. Matsumi and M. Kawasaki. *J. Chem. Phys.*, **95**, 6218 (1991).
12. E. E. Marinero, C. T. Rettner and R. N. Zare. *J. Chem. Phys.*, **80**, 4142 (1984).
13. V. R. McCrary, R. Lu, D. Zakheim, J. A. Russell, J. B. Halpern and W. M. Jackson. *J. Chem. Phys.*, **83**, 3481 (1985).
14. H. Okabe. *Photochemistry of Small Molecules*, A Wiley-Interscience, New York, p. 370 (1978).
15. M. Kh. Karapet'yants and M. K. Karapet'yants. *Handbook of Thermodynamic Constants of Inorganic and Organic Compounds*, Ann Arbor, London, p. 104–106, 194, 226, 231 (1970).
16. G. Black and L. E. Jusinski. *J. Chem. Phys.*, **82**, 789 (1985).
17. E. Zamir and R. D. Levine. *Chem. Phys.*, **52**, 253 (1982).